Optical and electronic-structure study of cubic and hexagonal GaN thin films

J. Petalas, S. Logothetidis, and S. Boultadakis
Department of Physics, Aristotle University of Thessaloniki, GR-54006 Thessaloniki, Greece

M. Alouani
Department of Physics, Ohio State University, Columbus, Ohio 43210-1368

J. M. Wills
Los Alamos National Laboratory, Los Alamos, New Mexico 87545
(Received 27 February 1995)

The optical properties of cubic and hexagonal GaN films in the region of the fundamental gap are studied with spectroscopic ellipsometry at temperatures between 110 and 630 K. It is verified that the gap of hexagonal GaN is higher than that of the cubic polytype. The parameters of the gaps are determined against temperature and the temperature shifts are found to be lower than and close to those of GaAs and GaP in the cases of cubic and hexagonal GaN, respectively. Additional theoretical calculations of the electronic structure of both polytypes using the full-potential linear-muffin-tin-orbital method reveal a significant contribution to the E_0 gap from the $8 \rightarrow 10$ transitions. The resulting gap energies are compared with the literature and the difference between the two GaN polytypes is discussed. The dielectric function $\varepsilon_2(\omega)$ is directly calculated from the band structure and its features at energies up to 9.5 eV are discussed and compared to experiment.

I. INTRODUCTION

GaN is a promising material for use in optoelectronic applications that operate in the near-UV region since it presents a large fundamental optical band gap at 3.4 eV. Up to now, various devices based on GaN and its solid solutions with AlN and InN have been developed, such as ultraviolet sensors,[1] blue- and UV-light-emitting diodes,[2] and optical-pumping structures,[3] photodetectors,[4] and heterostructure field-effect[5] transistors. The material was known to crystallize only in the hexagonal (wurtzite) form, which is thermodynamically stable. But, in the 1980s, a cubic, metastable form of the material was discovered during deposition on suitable substrates, such as GaAs(001), MgO(001), β-SiC(100), and Si(100). Total-energy calculations verified the high stability of the wurtzite phase, which is common in column-III nitrides.[6,7] The fundamental gap of both polytypes is of direct nature and hence the interest in their potential applications is now intense. The latter is followed by an interest from a theoretical point of view; thus, works on the electronic structure of the cubic polytype are increasingly being reported.

Since GaN is to be used in *optoelectronic* devices, the detailed knowledge of its optical behavior, especially with respect to temperature, is necessary. Some work has been done on the wurtzite (α-) modification,[8–12] whereas data on the cubic (β-) counterpart are scarce[11–14] and confined to the fundamental gap. Yet, considerable disagreements exist concerning the energy position of the fundamental gap of β-GaN, whereas its temperature dependence in the case of both polytypes is practically unknown. Recently, works have been published on the temperature dependence of the optical gaps above 5 eV,[15] and on some preliminary results on the fundamental gaps of α- and β-GaN.[16] Moreover, a modulated-photoreflectance study of the fundamental gap of β-GaN at temperatures up to 300 K has also been reported.[17] In view of the above, it is important to compare the optical responses of the cubic and hexagonal GaN polytypes in the region of the fundamental gap and examine their temperature dependence.

Therefore, in this work we present results on the optical properties of α- and β-GaN in the energy region of their fundamental optical band gap (1.5–6.3 eV) and as a function of temperature over the range 110–630 K, using the experimental technique *spectroscopic ellipsometry*, in an aim to determine and compare the respective energy locations of the gaps and their shifts with temperature. In parallel with the experiment, we perform electronic band-structure calculations with the full-potential linear-muffin-tin-orbital (FPLMTO) method in conjunction with the local-density approximation (LDA) in order to compare the calculated dielectric function of both polytypes with the experiment. The experimental details of the work are included in Sec. II and the theoretical models that are applied for the fitting of the experimental data are presented in Sec. III. In Sec. IV, are the results and discussion on the dielectric-function spectra (Sec. IV A), the gap location and temperature dependence (Sec. IV B), and the theoretical calculations (Sec. IV C). Finally, the conclusions of this work are summarized in Sec. V.

II. EXPERIMENTAL DETAILS

The GaN thin films were grown with electron-cyclotron-resonance molecular-beam epitaxy (ECR-MBE) using Ga vapor in an ECR-activated nitrogen atmosphere. The cubic polytype was grown on a Si(100)

0163-1829/95/52(11)/8082(10)/$06.00

surface, which, in contrsat to Si(111), is reported to lead to the formation of the zinc-blende structure.[18] The hexagonal polytype was grown on an Al_2O_3 (sapphire) substrate and exhibits wurtzite structure. The thicknesses of the α- and β-GaN samples was determined to be 4.0 and 0.7 μm, respectively, and their morphology was verified by several techniques, namely transmission and scanning electron microscopy, x-ray diffraction, and reflection high-energy electron diffraction.[16]

The experimental technique that was applied for the study of the optical properties is spectroscopic ellipsometry, a nondestructive technique that measures directly the complex dielectric function $\varepsilon(\omega)$ $[=\varepsilon_1(\omega)+i\varepsilon_2(\omega)]$ of bulk materials.[19] This quantity enabled the investigation of the electronic structure since $\varepsilon_2(\omega)$ is directly related to the point density of states for interband transitions.[20] The method has an advantage over other combined optical techniques, such as reflectivity and absorption, which determine $\varepsilon(\omega)$ indirectly. Ellipsometry measurements were performed in the photon energy region 1.5–6.3 eV using a rotating-analyzer ellipsometer and a Xe lamp as a light source. The specimens were placed inside a specially designed chamber that operated under ultrahigh-vacuum (UHV) conditions and allowed for heating of the sample under study, as well as cooling using liquid nitrogen. The system worked at temperatures between 110 and 620 K, and at 110 K the pressure in the chamber was around 6×10^{-9} mbar, which is low enough to avoid the formation of an ice layer on top of the samples. The angle of incidence of the light beam on the samples surface was 67.5° and all measurements were taken with a photon-energy interval of 5 meV. Before being placed inside the UHV chamber, the specimens were cleaned with a four-stage procedure that is reported to remove organic contaminants from the outer surface, namely, successive heating at 50 °C for 10 min in trichlorethylene, acetone, and methanol, and finally rinsing in deionized water.

III. THEORETICAL MODELING OF THE DIELECTRIC FUNCTION

A useful formalism to deduce the major parameters of optical gaps of crystalline materials, such as their energy location and broadening, is the model suggested in Ref. 20, which considers the experimentally measured $\varepsilon(\omega)$ spectra as a sum of contributions from all direct gaps and thus fits the derivative-spectra $[d\varepsilon(\omega)/d\omega$ and $d^2\varepsilon(\omega)/d\omega^2]$ line shapes appropriately. Yet, in the case of the fundamental gap of materials in thin-film form, the method cannot be applied, since the experimental dielectric-function spectra are dominated at photon energies below and around the gap by interference fringes, which result from the multiple reflection of light at the film/substrate interface and thus convey information on the substrate, as well. The fringes diminish rapidly in the region of the fundamental gap but nevertheless modify the line shape of $\varepsilon(\omega)$. Thus, in an aim to model the dielectric function, we employ the parabolic band model (PBM),[21,22] which assigns to the $\varepsilon(\omega)$ certain analytic line shapes, which depend on the type and nature [i.e., E_{ind}, E_0, E_0', E_1, E_1', or two dimensional (2D), 3D, etc.] of the observed gap.

The fundamental gaps of group-IV and III-V materials are usually of the type E_0 or E_0', which correspond in most cases to 3D minima (M_0 type) critical points (CP's). According to the PBM, the contribution of such CP's to the dielectric function is of the form

$$\varepsilon_1(\omega)-1=A_0[f_1(x_0)+\tfrac{1}{2}(\omega_0/\omega_{0S})^{3/2}f_1(x_{0S})]\ , \quad (1)$$

$$\varepsilon_2(\omega)=A_0[f_2(x_0)+\tfrac{1}{2}(\omega_0/\omega_{0S})^{3/2}f_2(x_{0S})]\ , \quad (2)$$

where ω_0 and ω_{0S} are the energies of gap and its spin-orbit counterpart, and x_0 (x_{0S}) is defined by the relation $x_0=\omega/\omega_0$ ($x_{0S}=\omega/\omega_{0S}$). The amplitude A_0 is expressed as $A_0=(4P^2/3)(2\mu^*/\omega_0)^{3/2}$, where P^2 is the average momentum matrix element and μ^* is the average reduced mass of the electron-hole pair. The inclusion of broadening modifies the above relations in a way that they resemble and reproduce better the experimentally observed line shapes. Namely, if we replace ω with the expression $\omega+i\Gamma$, the factors $f_1(x)$ and $f_2(x)$ of Eqs. (1) and (2) that are given in Ref. 21 become[22]

$$f_1(x,\gamma)=(x^2+\gamma^2)^{-2}\times\{(x^2-\gamma^2)[2-F(1+x,\gamma)-F(1-x,\gamma)]-2\gamma x[F(-x-1,\gamma)-F(x-1,\gamma)]\} \quad (3)$$

and

$$f_2(x,\gamma)=\frac{(x^2-\gamma^2)F(x-1,\gamma)-2\gamma xF(-x+1,\gamma)}{[1+(x^2+\gamma^2-1)H(x^2+\gamma^2-1)]^2} \quad (4)$$

where

$$F(x,\gamma)=\left[\frac{x+(x^2+\gamma^2)^{1/2}}{2}\right]^{1/2}$$

and

$$\gamma_0=\Gamma_0/\omega_0,\quad \gamma_{0S}=\Gamma_{0S}/\omega_{0S}\ .$$

In the case of GaN, the fundamental gap is of the E_0 type in both modifications and thus three parameters are needed for its description, namely A_0, E_0, and Γ_0.

Since at energies around 7 eV and above the higher gaps of the material are located,[15] a constant contribution from higher energies has also to be assumed for a correct modeling of the fundamental gap. This contribution may be considered to be a real constant greater than unity, ε_∞, and in this case the experimental dielectric-function spectra can be fitting using five parameters, namely, film thickness d, A_0, E_0, Γ_0, and ε_∞ (model 1). The contribution from the spin-orbit-split counterpart $E_0+\Delta_0$ is not considered separately but included in the E_0 gap line shape. This assumption does not cause any significant error in view of the facts that the amplitude of $E_0+\Delta_0$ is usually much lower than that of E_0 and that the experimental spectra are decisively modified by interference fringes that " hide" to some extent the spectral features of the film.

A more complex contribution can be also considered, namely, by substituting the contribution from all higher gaps with a mean gap, which has the form of a Lorentz oscillator and is centered at the center of gravity of the higher gaps. In the case of β-GaN there exist two neighboring higher gaps, E_1 and E_2, at energies between 6.8 and 8 eV that dominate the optical spectra.[13] Analysis of the gaps with the model proposed in Ref. 20 estimated their energies and broadenings at 6.920 and 7.571 eV and 314 and 89 meV, respectively.[15] Using these data, the energy location E_L of the mean gap can be found from the expression

$$E_L=\frac{\left[\left[\frac{A_1}{\Gamma_1}\right]E_1+\left[\frac{A_2}{\Gamma_2}\right]E_2\right]}{\left[\frac{A_1}{\Gamma_1}+\frac{A_2}{\Gamma_2}\right]}, \tag{5}$$

where A_i, E_i, and Γ_i $(i=1,2)$ are the amplitudes, energies, and broadenings of the two gaps.[23] The amplitudes A_1 and A_2 are estimated to be 0.997 and 0.521, respectively, and thus a value $E_L=7.342$ eV is deduced. The contribution of the mean gap to the dielectric function $\varepsilon_2(\omega)$ at energies below the fundamental gap E_0 is set to zero using a Heaviside step function $\Theta(y)$ and thus $\varepsilon_2(\omega)$ becomes

$$\varepsilon_2(\omega)=\frac{A_L\Gamma_L\omega}{(E_L^2-\omega^2)^2+\Gamma_L^2\omega^2}\theta(\omega/\omega_0),$$

$$\text{where } \theta(y)=\begin{cases}0 & \text{for } y<1\\ 1 & \text{for } y>1\end{cases}. \tag{6}$$

In an aim to perform meaningful fits to the experimental spectra, one should use the minimum possible number of free parameters and thus E_L can be assumed of fixed value. Therefore, the dielectric function of β-GaN in the energy region of the fundamental gap can be fitted with six parameters, namely, thickness d, A_0, E_0, Γ_0, A_L, and Γ_L (model 2).

As will be demonstrated in the following section, the dielectric-function spectra of α-GaN exhibit a strong feature in the region of the gap, which could be of excitonic origin. The Fano-profile line shape that describes an exciton is of the form[20]

$$\varepsilon_{\text{exc}}(\omega)=C-A_x/(\omega-E_x+i\Gamma_x), \tag{7}$$

where A_x, E_x, and Γ_x are the amplitude, energy location, and broadening of the exciton, and C is a complex constant background. In order to minimize the free parameters involved, we select in this case to fit the absorption coefficient spectra, which are created by the dielectric-function experimental spectra, by considering the superposition of an E_0 gap [Eqs. (1) and (2)] and an exciton [Eq. (7)]. Since the distance ΔE_x between the direct gap exciton and the gap itself is reported to be around 28 meV,[24] it can be assumed constant and around 20 meV and thus E_x is directly related to E_0 via the expression $E_x=E_0-\Delta E_x$. The fits can extend in the energy region above the diminishing of interference fringes and thus the absorption spectra of α-GaN can be fitted using six free parameters, namely, A_0, E_0, Γ_0, A_x, Γ_x, and C_{abs}, where C_{abs} is a constant (model 3).

IV. RESULTS AND DISCUSSION

A. Dielectric-function spectra

The pseudodielectric-function spectrum of the β-GaN thin film grown on Si at various temperatures in the energy region of the fundamental energy gap is presented in Fig. 1. The low-energy part of the spectrum is dominated by interference fringes, which result from the multiple reflection of the incident light beam at the interface between the film and the substrate. The fringes at redshifted with temperature, a fact suggesting that the energy gap is lower at high temperatures, as observed in all group-IV elements and III-V compounds. The amplitude of the interference fringes around the gap is reduced at high temperatures, a fact indicating that the broadening of the fundamental gap increases with temperature.

The spectra of the real $[\varepsilon_1(\omega)]$ and the imaginary $\varepsilon_2(\omega)$ parts of the pseudodielectric function of the α-GaN thin film grown on sapphire in the energy region of the fundamental energy gap are shown in Figs. 2(a) and 2(b), respectively, at various temperatures. Similarly with β-GaN, the multiple reflection of light at the film/substrate interface induces interference fringes at the lower-energy part of the spectrum. The fringes are narrow compared to β-GaN (Fig. 1), because the thickness of the α-GaN film is much higher ($\approx$4.0 μm) than that of the β-GaN film ($\approx$0.7 μm). From the spectra, it can be seen that increasing temperature causes a redshift of the fundamental gap energy and an increase of its broadening.

The amplitude and line shape of the interference fringes observed in Figs. 2(a) and 2(b) suggest that there is a further contribution to $\varepsilon(\omega)$, apart from that estimated theoretically by considering a layered configuration (air/film/substrate).[19] This can be verified, e.g., by the high average value of $\varepsilon_2(\omega)$ in the energy region below 3.3 eV, where the GaN film is transparent. This observa-

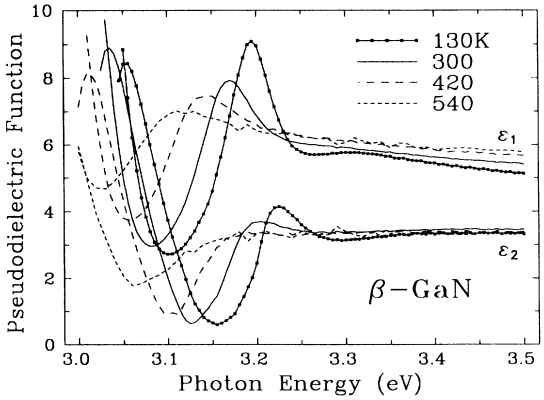

FIG. 1. The real (ε_1) and imaginary (ε_2) parts of the pseudodielectric function of a cubic GaN (β-GaN) thin film grown on silicon in the energy region of the fundamental energy gap at various temperatures.

tion can be attributed to the finite thickness of the sapphire substrate, which causes a part of the incident light beam to be reflected at the back surface of the substrate and emerge from the front surface having become incoherent and thus providing a constant light background. Furthermore, the systematic amplitude decrease of the interference fringes can be ascribed to nonuniformities in the layered structure in the region of the GaN/sapphire interface, which cause partial depolarization of the reflected light.[25]

B. Gap location and temperature dependence

In the case of β-GaN, the film/substrate system can be modeled using the relations for reflection from layered structures[19] and thus the dielectric-function spectra (see Fig. 1) can be fitted assuming an E_0 line shape for the fundamental gap and a constant contribution ε_∞ from higher energies (model 1, see Sec. III). A typical fit to the real and imaginary parts of the pseudodielectric function is shown with the solid lines in Figs. 3(a) and 3(b), respectively, with the experimental spectrum designated with the solid-dotted lines. The energy region of the fit is that shown in Fig. 3, and is selected so as to include contributions from the transparent as well as absorbing energy regions of the GaN material. The gap energy at room-temperature (RT) (300 K) is estimated to 3.188 (19) eV, with respective broadening 35 (4) meV. The numbers in parentheses indicate the 95% confidence limits.

The energy location of the E_0 gap of β-GaN, which is determined by the above fitting of the pseudodielectric function is plotted against temperature in Fig. 4 with solid circles. The gap is lowered with temperature and its temperature shift λ ($=-dE_0/dT$) between 250 and 600 K is found to be 3.67 (1) $\times 10^{-4}$ eV/K. The above are fitted with an average Bose-Einstein statistical factor[26] (solid line, Fig. 4), which assumes that the crystal phonons have a mean energy Ω, which leads to a mean frequency $\Theta=\Omega/k_B$

$$E(T)=E_B-a_B\left[1+\frac{2}{e^{\theta/T}-1}\right], \tag{8}$$

as well as with the empirical Varshni approximation[27] (dashed line, Fig. 4)

$$E(T)=E_0-\frac{aT^2}{T+\beta}. \tag{9}$$

As described in Sec. III, the pseudodielectric-function

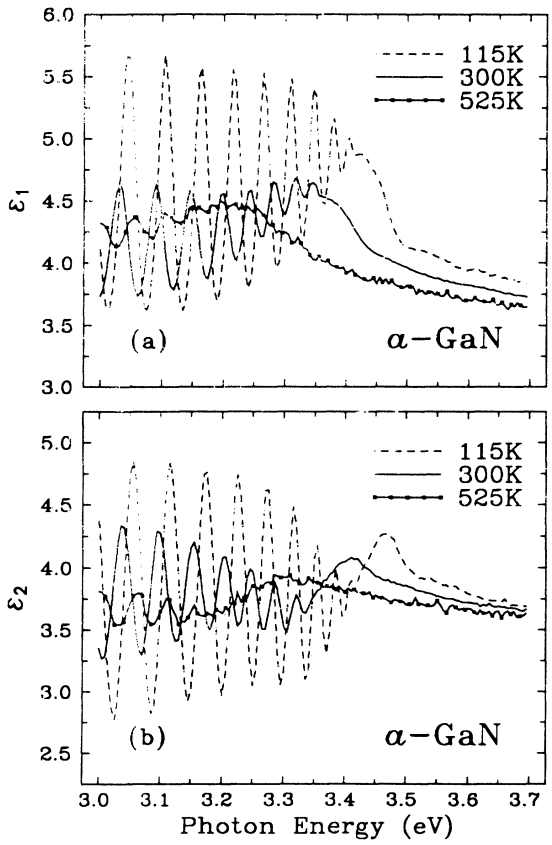

FIG. 2. The real (a) and imaginary (b) parts of the pseudodielectric function of a hexagonal GaN (α-GaN) thin film grown on sapphire in the energy region of the fundamental energy gap at various temperatures.

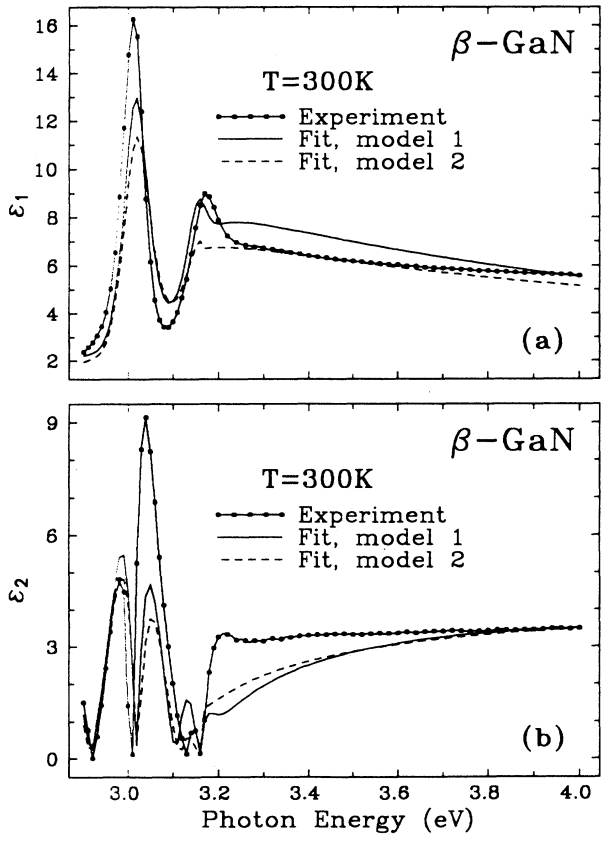

FIG. 3. Typical fits (solid and dashed lines) to the real (a) and imaginary (b) parts of the pseudodielectric function (solid-dotted line) of cubic GaN in the energy region of the fundamental gap using models 1 and 2 (see Sec. III), respectively, at 300 K.

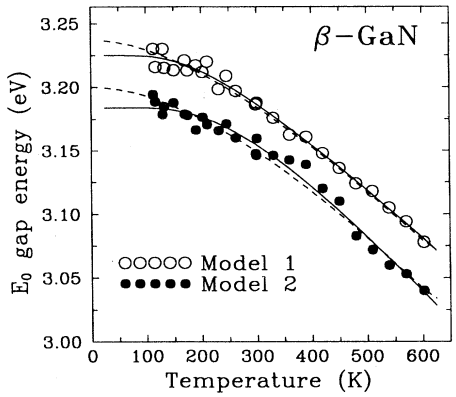

FIG. 4. Temperature dependence of the energy position of the E_0 gap of the cubic GaN (open and solid circles). The energy values shown refer to analysis using models 1 and 2, respectively (see Sec. III). The solid and dashed lines represent fits to the data with Eqs. (8) and (9), respectively.

spectra of β-GaN are also fitted assuming an E_0 CP superimposed on a complex contribution from higher energies that is approximated by that of a Lorentz oscillator (model 2). A typical fit corresponding to $T=300$ K is shown in Fig. 3 with the dashed lines. The values of the energy location of the E_0 CP are plotted against temperature in Fig. 4 with the open circles. The gap is located at RT at 3.160 (80) eV and its broadening is 38 (15) meV. The estimated 95% confidence limits, which are shown in parentheses, are significantly larger than the corresponding ones deduced by model 1, because model 2 involves one more free parameter than model 1. A further reason is that the background contribution of model 1 affects only the real part of the dielectric function, whereas the contribution considered in model 2 influences both $\varepsilon_1(\omega)$ and $\varepsilon_2(\omega)$. The values of the energy location of the fundamental gap, which are estimated by model 2, are systematically higher by $\approx$40 meV than those deduced by model 1, a discrepancy that is attributed to the models themselves. The energy location of the fundamental gap (around 3.17 eV at RT, considering the joint results of models 1 and 2) compares well to the data reported by Powell *et al.*[12] [3.21 (2) eV] and Ramirez-Flores *et al.*[17] (3.235 eV), who used optical absorption and modulated photoreflectance measurements, respectively.

The temperature shift λ of the E_0 gap of β-GaN between 250 and 600 K is estimated in the case of model 2 at 3.7 (4)$\times 10^{-4}$ eV/K and thus is almost identical to that found using model 1. The fits to the experimental points produced by model 2 and using Eqs. (8) and (9) are shown in Fig. 4 with solid and dashed lines, respectively. The values of the best-fit parameters, which are determined by Eqs. (8) and (9) using models 1 and 2, are listed in Table I. The numbers in parentheses indicate the 95% confidence limits. As can be seen in Table I, the values of the Debye temperatures Θ, which are determined from the fits, are similar [around 600 (150) and 800 (180) K for models 1 and 2, respectively], but are in good agreement with the literature, since the Debye temperature of α-GaN is estimated to be 600 K,[28] whereas the parameter Θ was evaluated to $\approx$500 K in the cases of the two higher gaps E_1 and E_2 of the material.[15] The values of the parameter α differ by 15% between models 1 and 2 [5.16 (24) and 6.06 (38)$\times 10^{-4}$ eV/K, respectively], and compare satisfactorily with the corresponding value deduced in Ref. 17 (6.697×10^{-4} eV/K). A reason for the observed discrepancy is the different temperature region of the corresponding fits (10–300 K in Ref. 17 and 110–600 K in our case). On the other hand, a direct comparison between the fits presented in Ref. 17 and this work can be accomplished if one considers the temperature coefficient $-dE_0/dT$ in the region from 100 to 300 K. Thus, its corresponding values are found to be around 2.5 and 2.1 (4)$\times 10^{-4}$ eV/K, from the results of Ref. 17 and this work, respectively, which compare well. The temperature shift $-dE_0/dT$ of the E_0 gap is shown in Table II in the case of the zinc-blende Ga-V compounds.[29,30] The two regions have to be distinct, namely, between 100 and 300 K and between 300 and 500 K, because the corresponding slopes are different. It is observable that β-GaN exhibits lower-temperature coefficients than GaAs and GaP in both temperature regions. The hexagonal polytype although exhibits higher-temperature coefficients than its cubic counterpart with values similar to those of GaAs and GaP.

The broadening parameter of the fundamental gap of β-GaN was found to increase with temperature. For example, in Fig. 5 we present with open circles the temperature dependence of the broadening parameter, which was determined in the region 100–600 K using model 2. The data are fitted according to the Bose-Einstein model,[25] which for the case of phonon-induced lifetime broadenings takes the form

$$\Gamma(T)=\Gamma_1+\Gamma_0\left[1+\frac{2}{e^{\theta/T}-1}\right]. \tag{10}$$

The first term in this expression represents the broadening invoked from temperature-independent mechanisms, such as impurity and surface scattering, electron-electron

TABLE I. Values of the parameters obtained by fitting the temperature dependence of the energies of the E_0 gap of cubic (β-) and hexagonal (α-) GaN with Eqs. (8) and (9). The numbers in parentheses indicate the 95% confidence limits.

	Model	E_B (eV)	a_B (eV)	Θ (K)	E_0 (eV)	α (10^{-4} eV/K)	β (K)
β-GaN	1	3.351 (39)	0.126 (43)	607 (132)	3.237 (3)	5.16 (24)	600 (fixed)
	2	3.394 (85)	0.210 (88)	818 (185)	3.200 (45)	6.06 (38)	800 (fixed)
α-GaN	3	3.725 (305)	0.236 (332)	692 (61)	3.510 (3)	8.58 (17)	700 (fixed)

TABLE II. Temperature coefficients ($-dE_0/dT$) of the critical-point energies of the E_0 gap of the zinc-blende Ga-V compounds in the temperature regions 100–300 K and 300–500 K (in 10^{-4} eV/K). The corresponding data for α-GaN are also noted. The numbers in parentheses designate the 95% confidence limits.

	GaAs	GaP	β-GaN		α-GaN
100–300 K	3.9 (9)[a]	5.0 (2)[c]	2.1 (4)[d]	2.5[e]	3.0 (2)[d]
300–500 K	5.0 (1.2)[b]	6.5 (6)[c]	3.4 (2)[d]		5.6 (2)[d]

[a]See Ref. 29.
[b]See Ref. 29, 400–500 K.
[c]See Ref. 30 and references therein.
[d]See this work.
[e]See Ref. 17.

interaction, and Auger processes, whereas the second term is caused by the electron-phonon interaction. The fit to the data with Eq. (10) was accomplished considering the temperature parameter Θ to have a fixed value of 800 K for compatibility with the energy-location results presented above. The fit is presented in Fig. 5 with the solid line. A projection of the fit line to $T=0$ K yields the zero-point broadening, which is estimated to 34.5 meV. The temperature coefficient $d\Gamma_0/dT$ in the region between 300 and 600 K, where the dependence becomes linear, is estimated to 0.13 meV/K. This value is around that of the E_2 gap[15] (0.12 meV/K) but much lower compared to that of the E_1 gap[15] (0.34 meV/K). This difference may be due to the possibly complex nature of the E_1 gap of β-GaN, in contrast with other Ga-V compounds, as discussed in Ref. 15.

As already discussed, in the case of α-GaN we selected to fit the pseudoabsorption coefficient $\alpha(\omega)$ spectra, which exhibits the features present in the pseudodielectric function and is calculated by the measured $\varepsilon_1(\omega)$ and $\varepsilon_2(\omega)$ spectra [Figs. 2(a) and 2(b)]. The large film thickness (around 4.0 μm) does not allow the interference fringes to distort the line shape around the gap significantly, as in the case of the β-GaN film. A typical spectrum of $\alpha(\omega)$ that corresponds to temperature $T=230$ K is presented in Fig. 6 (solid-dotted line). The rapid rise of $\alpha(\omega)$ at energies immediately after the diminishing of the interference fringes forms a distinct peak and exhibits the line shape of an excitonic structure, otherwise known as a Fano profile. Therefore, we selected to fit the pseudoabsorption coefficient spectra of α-GaN assuming the joint contribution of an E_0 gap and an exciton situated 20 meV below the E_0 gap (model 3, see Sec. III). The corresponding fit to the experimental data is shown in Fig. 6 with the solid line. The fit represents well the rise of absorption and the subsequent exciton line shape. If the distance between the E_0 gap and the exciton is set anywhere in the range 15–25 meV, fits of similar quality are achieved.

The values of the energy location of the exciton gap of α-GaN, which are determined using model 3 are shown against temperature in Fig. 7 with the solid circles. The E_0 gap is located at RT at 3.437 (12) eV, thus, the corresponding exciton is situated 20 meV lower, at 3.417 eV. In the energy region that is being fitted, the $\alpha(\omega)$ spectra are dominated by the exciton; thus, a parameter with physical significance is the exciton broadening Γ_x, which is estimated to 50 (18) meV at RT. The temperature dependence of the exciton energy of α-GaN is shown in Fig. 7, with solid circles. The solid and dashed lines designate fits to the data with Eqs. (8) and (9). The corresponding temperature dependence of the E_0 gap is the same, since the distance between the E_0 gap and the exciton is fixed to 20 meV. The values of the best-fit parameters are listed in Table I. The Debye temperature Θ was estimated to 690 K, which is near the value given in the literature (600 K,[24] and between the values estimated for β-GaN in the cases of models 1 and 2 (600 and 800 K, respectively). α-GaN exhibits a stronger temperature dependence than its zinc-blende counterpart: This difference is verified by the value of the parameter α (8.58×10^{-4} eV/K for α-GaN) as well as the temperature shift λ between 300 and 600 K, which is calculated to be

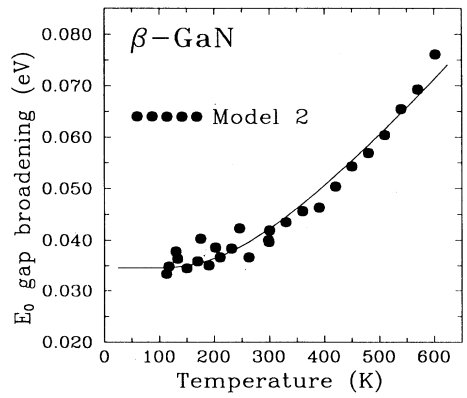

FIG. 5. Temperature dependence of the broadening parameter of the E_0 gap of cubic GaN (solid circles). The broadening values shown refer to analysis using model 2 (see Sec. III). The solid line represents the fit to the data with Eq. (10).

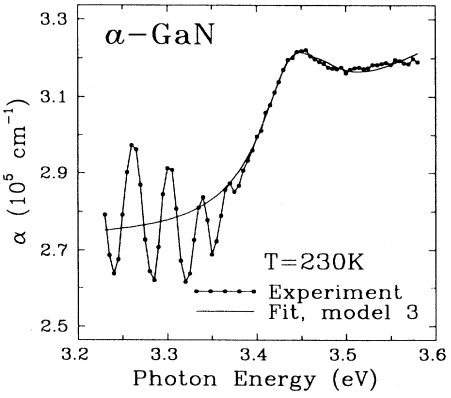

FIG. 6. Typical fit (solid line) of the pseudoabsorption coefficient spectrum (solid-dotted line) of hexagonal GaN in the energy region of the fundamental gap using model 3 (see Sec. III) at 230 K.

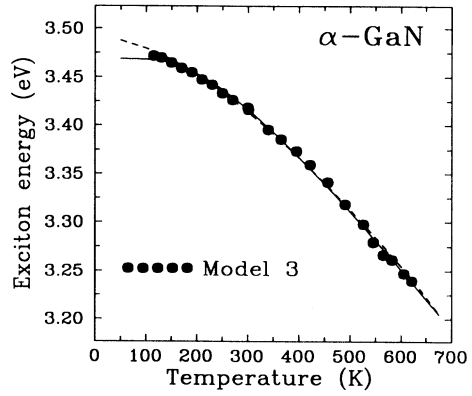

FIG. 7. Temperature dependence of the energy position of the exciton associated with the E_0 gap of hexagonal GaN (solid circles). The energy values shown refer to analysis using model 3 (see Sec. III). The solid and dashed lines designate fits to the data with Eqs. (8) and (9), respectively.

5.64×10^{-4} eV/K and is much larger than the corresponding value for β-GaN (3.57×10^{-4} eV/K).

The dependence of the broadening parameter Γ_x of the exciton below the E_0 gap of α-GaN against temperature is shown in Fig. 8 with solid circles. The solid line is the fit to the data with Eq. (10) assuming that the Debye temperature Θ is fixed to 700 K, for compatibility with the corresponding results for the E_0 gap energy. The zero-point broadening $\Gamma_x(0)$ is 39.5 meV. The temperature coefficient $d\Gamma_x/dT$ in the region between 300 and 600 K, where its dependence becomes linear, is estimated to 0.17 meV/K, this value is around that for the E_0 gap ($d\Gamma_0/dT=0.13$ meV/K) of β-GaN.

Finally, in Table III we present the values for the fundamental energy gap of β- and α-GaN at RT, which are estimated in this and other works. It is clearly seen that the cubic phase exhibits a gap lower in energy than the wurtzite one. This difference occurs systematically between the zinc-blende (ZB) and wurtzite (WU) polytypes of materials and is explained theoretically. In detail, the Γ_{1v} and Γ_{1c} band edges in the wurtzite structure repel only weakly because their parent zinc-blende states (Γ_{15v} and Γ_{1c}, respectively) have different orbital characters (namely p-d and s). Yet, this upward repulsion of Γ_{1v} is partially canceled by a crystal-field splitting of the valence band. The resulting net effect is an increase of the bands separation at Γ in the WU structure, with respect to the ZB one.[31]

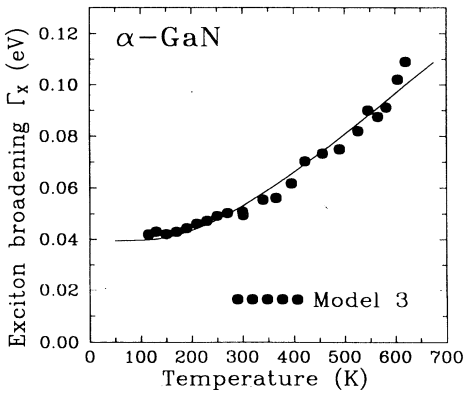

FIG. 8. Temperature dependence of the broadening parameter of the exciton associated with the E_0 gap of hexagonal GaN (solid circles). The broadening values shown refer to analysis using model 3 (see Sec. III). The solid line designates the fit to the data with Eq. (10).

C. Theoretical predictions and comparison with experiment

The electronic band-structure calculations on β- and α-GaN are based on the LDA with an all-electron scalar-relativistic FPLMTO basis set, as described in Ref. 32. The electronic band structure of β-GaN along the major symmetry lines of the Brillouin zone is presented in Fig. 9. The arrow in the figure indicates the fundamental gap of the material. The absolute value of the fundamental gap is underestimated compared to the experimental data. This is typical of the use of the LDA. The addition of a suitable external potential can empirically tune the conduction-band states and bring the gap value close to experiment.

The calculated energy values of the first direct gaps of the ZB structure at the major symmetry points of the Brillouin zone along with the fundamental gap of the wurtzite structure are listed in Table IV. The results are compared with corresponding LDA-based calculations on both polytypes that are found in the literature (Table IV). In detail, we present the data reported by Christensen and Gorczyca[33] and Rubio *et al.*[34] which are produced with LDA-based calculations. There is good agreement between the results, especially concerning the higher direct gaps of β-GaN, where the differences are of the order of 0.2 eV. The adjustment of the conduction bands so as to coincide with the experiment at the Γ point is expected to shift the energy values of all gaps but not to affect the location of the higher gaps so significantly as observed in the case of SiC.[35] All calculations estimate the fundamental gap of α-GaN to be higher than that of β-GaN, in agreement with the theoretical predictions. It should be also mentioned that the calculations of Bloom *et al.*[9] estimate the gap of α-GaN higher (100 meV) than that of β-GaN. The directness of the Γ_{1v}-Γ_{1c} gap is preserved even in the ZB form of GaN, since the high atomic number of Ga creates a strong potential at the nucleus, which affects the Γ_{1c} state.[36] The latter is quite sensitive to the depth of the potential near the nucleus and, therefore, is located lower in energy with respect to conduction-band states at other k points. The fact that L_{1c} is well above Γ_{1c} in β-GaN ensures that the fundamental gap of the wurtzite polytype will be also of direct nature.[31]

The self-consistent energy eigenvalues (Fig. 9) and wave functions are directly used to evaluate the imaginary part $\varepsilon_2(\omega)$ of the dielectric function. In Figs. 10(a) and 10(b), we present the calculated $\varepsilon_2(\omega)$ spectra of β- and α-GaN, respectively, (solid lines) for $E\perp c$ at energies up to 9.5 eV. The corresponding experimental spectra

TABLE III. Comparison between the values of the fundamental gaps (in eV) of β- and α-GaN at room temperature reported in the literature. The experimental techniques used are also noted. The numbers in parentheses indicate the 95% confidence limits.

	Ref.	β-GaN	α-GaN	Technique
This work		3.17 (2)	3.44 (1)	ellipsometry
Ramirez-Flores *et al.*	17	3.23		modulated photoreflectance
Okumura, Yoshida, and Okanisa	11	3.37	3.54	reflection
Powell	12	3.21	3.45	cathodoluminescence
Sitar	13	3.28	3.44	photoluminescence
Strite	14	3.45		cathodoluminescence

(this work and Ref. 15) are shown with the dashed lines. The respective energy locations of the fundamental gap differ between theory (1.8 and 2.15 for β- and α-GaN, respectively) and experiment (3.17 and 3.44 eV) due to the application of the LDA, as mentioned above. The spectra compare well to those calculated by LDA-LMTO in the atomic sphere approximation (Ref. 33).

In the case of β-GaN, the calculated fundamental gap is found to lie at 1.8 eV. The band-to-band contributions to the $\varepsilon_2(\omega)$ in the region of the fundamental gap are shown in the inset of Fig. 10(a). It is clearly seen that not only the $9\rightarrow 10$, but also the $8\rightarrow 10$ interband transitions contribute to the gap. This is in contrast to what is reported in the case of GaAs,[37,38] where the strength of the $3\rightarrow 5$ transitions is considerably weaker than that of the $4\rightarrow 5$ ones in the region of the gap and similar with the case of diamond,[39] where the $3\rightarrow 6$ transitions are found to contribute significantly to the E_0' gap. Above the fundamental gap, the calculated $\varepsilon_2(\omega)$ of β-GaN exhibits three distinct features at energies up to 8 eV. The first appears as a distinct peak at 5.6 eV, whereas the other two (situated at 6.3 and 7.2 eV, respectively) form a single broad structure. An LDA correction of the calculations is not expected to shift uniformly the observed gaps towards higher energies and thus may move the calculated 5.6- and 6.3-eV gaps towards the experimental 7.0-eV peak, as well as shift the third calculated gap at 7.2 eV only slightly, so as to coincide with the 7.5-eV experimental feature. In this way, theory would match the experiment in terms of peaks number and location.

The experimental spectrum[15] [dashed line, Fig. 10(a)] is dominated above the fundamental gap by a broad structure that consists of two peaks centered at 7.0 and 7.6 eV. These peaks are thought to correspond to the E_1 and E_2 structures of the material and are designated E_{1C} and E_{2C} in Fig. 10(a). The experiment cannot distinguish between the 5.6- and 6.3-eV peaks and observes them as a single broad structure. This may explain why the estimated broadening parameter of the 7.0-eV peak is found to be surprisingly large, compared to that at 7.6 eV.[15] In most III-V compounds, the E_1 structure is attributed mainly to interband electronic transitions around the L point and along the $\langle 111\rangle$ (Λ-) direction of the Brillouin zone. In view of the above, a calculation of the individual contributions to the E_{1C} structure would provide valuable insight on whether other regions of k space contribute to E_{1C} as well and thus increase its broadening. Finally, the 7.2-eV structure of the calculated $\varepsilon_2(\omega)$ corresponds to the E_{2C} peak refers to the E_2 gap of the material, which is occurring around the X point.

The calculated $\varepsilon_2(\omega)$ spectrum of α-GaN [solid line in Fig. 10(b)] is also rich in features at energies above the fundamental gap. One can distinguish two neighboring peaks, situated at 5.8 and 6.5 eV, which corresponds to the experimentally observed peak at 6.8 eV [dashed line, Fig. 10(b)] that is designated E_{1H}. The 5.8- and 6.5-eV peaks are assigned mainly to transitions at the M point and the M-L line.[15,33] Higher than 7.3 eV, the calculated $\varepsilon_2(\omega)$ spectrum exhibits a doublet (7.6 and 8.1 eV, respectively), which corresponds to the experimental peak at 7.8 eV. This doublet is attributed to the M and H points,[15] whereas a contribution from the Σ direction is also suggested in the literature.[33]

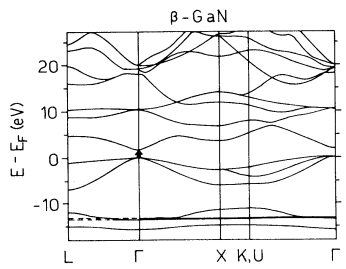

FIG. 9. Electronic band-structure calculation of zinc-blende GaN with the LDA-based full-potential LMTO method. The arrow designates the location of the fundamental gap.

TABLE IV. Comparison between the calculated critical-point energies (in eV) of the first direct gaps of zinc-blende (β-) GaN at the major symmetry points of the Brillouin zone and other LDA-based calculations found in the literature. The corresponding results for the fundamental gap of wurtzite (α-) GaN are also listed.

		This work	Ref. 33	Ref. 34
β-GaN	Γ_v-Γ_c	1.8	2.18	2.1
	L_v-L_c	5.8	5.9	6.0
	X_v-X_c	6.3	6.1	6.0
	K_v-K_c	7.5	7.3	7.3
α-GaN	Γ_v-Γ_c	2.15	2.45	2.3

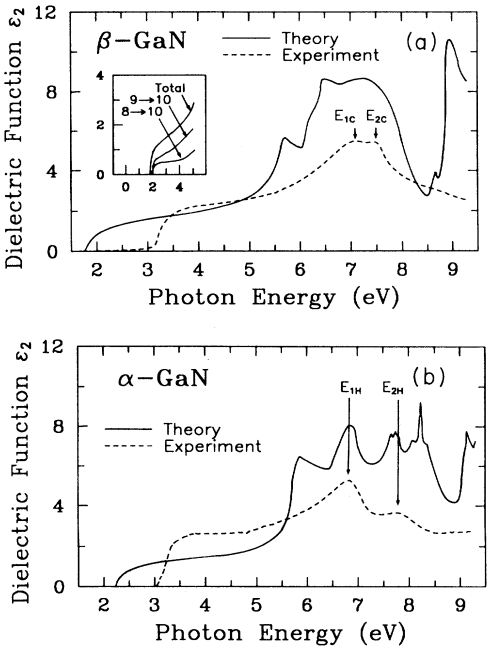

FIG. 10. Calculated dielectric-function $\varepsilon_2(\omega)$ spectra (solid lines) of β- (a) and α- (b) GaN. The dashed lines designate the corresponding experimental $\varepsilon_2(\omega)$ spectra. The arrows in (a) indicate the location of structure in the spectra. Inset of (a): The band-to-band contributions to the dielectric function $\varepsilon_2(\omega)$ around the fundamental gap of β-GaN.

V. SUMMARY

We measured thin films of zinc-blende and wurtzite GaN in the energy region of the fundamental energy gap at various temperatures between 110 and 630 K. We developed appropriate models to fit the dielectric-function spectra and deduced the locations and broadenings of the gaps against temperature. The gaps can be well represented with E_0-type line shapes and, in the case of α-GaN, an excitonic contribution is evident in the spectra. At 300 K, the gaps are located at 3.17 and 3.44 eV for β- and α-GaN, respectively, values which compare well with the literature. The observed difference in the location of the gaps and their directness are discussed in terms of their conduction-band characteristics. The temperature shifts of the gaps are determined and it is discovered that the gap of α-GaN exhibits a significantly stronger dependence than β-GaN. The temperature dependence of β-GaN is found to be generally small compared to other Ga-V compounds.

Furthermore, electronic-structure calculations with LDA-FPLMTO estimate the gaps of β- and α-GaN at 1.8 and 2.15 eV, respectively, and compare well with other LDA-based calculations. A band-to-band contribution analysis yields that, apart from the $9\rightarrow 10$ interband transitions, the $8\rightarrow 10$ ones contribute decisively to the fundamental gap of β-GaN, similarly to what is observed for diamond. The calculated $\varepsilon_2(\omega)$ spectra in the energy region up to 10 eV are richer in features than the experimental ones. The respective features are compared and assigned to critical points in the Brillouin zone. The proximity of two neighboring peaks in the calculated spectra of β-GaN that are attributed to the E_1 structure provides evidence on the large broadening of this structure, a fact that was verified by experiment.

ACKNOWLEDGMENTS

The authors are thankful to Professor T. D. Moustakas for kindly providing the GaN specimens and grateful to K. Konstantinidis for his technical assistance. This work was financially supported in part by the Human Capital and Mobility Programme, under Contract No. CHGE-CT93-0027, and the Greek General Secretariat for Research and Technology. M.A. acknowledges the partial support provided by the Department of Energy, Basic Energy Sciences, Division of Materials Sciences, and the supercomputer time provided by the Ohio supercomputer.

[1]M. Asif Khan, J. N. Kuznia, D. T. Olson, J. M. Van Hove, M. Blasingame, and L. F. Reitz, Appl. Phys. Lett. **60**, 2917 (1992).

[2]S. Nakamura, M. Senoh, and T. Mukai, Appl. Phys. Lett. **62**, 2390 (1993).

[3]H. Amano, T. Tanaka, Y. Kunii, K. Kato, S. T. Kim, and I. Akasaki, Appl. Phys. Lett. **64**, 1377 (1994).

[4]R. P. Joshi, A. N. Dharamsi, and J. McAdoo, Appl. Phys. Lett. **64**, 3611 (1994).

[5]M. Asif Khan, J. N. Kuznia, D. T. Olson, W. J. Schaff, J. W. Burm, and M. S. Shur, Appl. Phys. Lett. **65**, 1121 (1994).

[6]C.-Y. Yeh, Z. W. Lu, S. Froyen, and A. Zunger, Phys. Rev. B **45**, 12 130 (1992).

[7]C.-Y. Yeh, Z. W. Lu, S. Froyen, and A. Zunger, Phys. Rev. B **46**, 10 086 (1992).

[8]B. Dingle, D. D. Sell, S. E. Stokowski, and M. Ilegems, Phys. Rev. B **4**, 1211 (1971).

[9]S. Bloom, G. Harbeke, E. Meier, and I. B. Ortenburger, Phys. Status Solidi B **66**, 161 (1974).

[10]C. G. Olson, D. W. Lynch, and A. Zehe, Phys. Rev. B **24**, 4629 (1981).

[11]H. Okumura, S. Yoshida, and T. Okahisa, Appl. Phys. Lett. **64**, 2997 (1994).

[12]R. C. Powell, N.-E. Lee, Y.-W. Kim, and J. E. Greene, J. Appl. Phys. **73**, 189 (1993).

[13]Z. Sitar, M. J. Paisley, J. Ruan, J. W. Choyke, and R. F. Davis, J. Mater. Sci. Lett. **11**, 261 (1992).

[14]S. Strite, J. Ruan, Z. Li, A. Salvador, H. Chen, D. J. Smith, W. J. Choyke, and H. Morkoc, J. Vac. Sci. Technol. B **9**, 1924 (1991).

[15]S. Logothetidis, J. Petalas, M. Cardona, and T. D. Moustakas, Phys. Rev. B **50**, 18 017 (1994).
[16]S. Logothetidis, J. Petalas, M. Cardona, and T. D. Moustakas, Mater. Sci. Eng. B **29**, 65 (1995).
[17]G. Ramirez-Flores, H. Navarro-Contreras, A. Lastras-Martinez, R. C. Powell, and J. E. Greene, Phys. Rev. B **50**, 8433 (1994).
[18]T. D. Moustakas, T. Lei, and R. J. Molnar, Physica B **185**, 36 (1993).
[19]See, e.g., R. M. A. Azzam and H. M. Bashara, *Ellipsometry and Polarized Light* (North-Holland, Amsterdam, 1977).
[20]M. Cardona, *Modulation Spectroscopy* (Academic, New York, 1969).
[21]S. Adachi, Phys. Rev. B **35**, 7454 (1987).
[22]A. D. Papadopoulos and E. Anastassakis, Phys. Rev. B **43**, 5090 (1991).
[23]S. Logothetidis and G. Kiriakidis, J. Appl. Phys. **64**, 2389 (1989).
[24]*Semiconductors. Physics of Group IV Elements and III-V Compounds,* edited by K.-H. Hellwege and O. Madelung, Landolt-Börnstein, New Series, Group III, Vol. 17 (Springer-Verlag, Berlin, 1982).
[25]M. Garriga, P. Lautenschlager, M. Cardona, and K. Ploog, Solid State Commun. **61**, 157 (1987).
[26]L. Vina, S. Logothetidis, and M. Cardona, Phys. Rev. B **30**, 1979 (1983).
[27]Y. P. Varshni, Physica (Utrecht) **34**, 149 (1967).
[28]E. Edjer, Phys. Status Solidi A **6**, K39 (1971).
[29]P. Lautenschlager, M. Garriga, S. Logothetidis, and M. Cardona, Phys. Rev. B **35**, 9174 (1987).
[30]S. Zollner, M. Garriga, J. Kircher, J. Humlicek, M. Cardona, and G. Neuhold, Phys. Rev. B **48**, 7915 (1993).
[31]C.-Y. Yeh, S.-H. Wei, and A. Zunger, Phys. Rev. B **50**, 2715 (1994).
[32]M. Alouani, J. W. Wilkins, R. C. Albers, and J. M. Wills, Phys. Rev. Lett. **71**, 1415 (1993).
[33]N. E. Christensen and I. Gorczyca, Phys. Rev. B **50**, 4397 (1994).
[34]A. Rubio, J. L. Corkill, M. L. Cohen, E. L. Shirley, and S. G. Louie, Phys. Rev. B **48**, 11 810 (1993).
[35]S. Logothetidis, H. M. Polatoglou, J. Petalas, D. Fuchs, and R. L. Johnson, Physica B **185**, 392 (1993).
[36]W. R. L. Lambrecht and B. Segall, in *Wide Band-Gap Semiconductors,* edited by T. D. Moustakas, J. J. Pankove, and Y. Hamakawa, MRS Symposia Proceedings No. 242 (Materials Research Society, Pittsburgh, 1992), p. 367.
[37]M. Alouani, L. Brey, and N. E. Christensen, Phys. Rev. B **37**, 1167 (1988).
[38]S. Logothetidis, M. Alouani, M. Garriga, and M. Cardona, Phys. Rev. B **41**, 2959 (1990).
[39]S. Logothetidis, J. Petalas, H. M. Polatoglou, and D. Fuchs, Phys. Rev. B **46**, 4483 (1992).